(1) Upper Limits to the Quiet-Time Solar Neutron Flux from 10 to 100 MeV.

(10) Shin/Moon, George M./Simnett[redacted] R. Stephen/White

Department of Physics and Institute of Geophysics and Planetary Physics

University of California
Riverside, California

(11) 23 June[redacted]75 (12) 31 p.

(14) IGPP-UCR-75-15

(15) N00014-69-A-0200-5004[redacted], NGR-05-008-022

The UCR large area solid-angle double scatter neutron telescope was flown to search for solar neutrons on 3 balloon flights on September 26, 1971, May 14, 1972 and September 19, 1972. The first two flights were launched from Palestine, Texas and the third from Cape Girardeau, Missouri. The float altitude on each flight was at about 5 g/cm^2 residual atmosphere. Neutrons from 10 to 100 MeV were measured. No solar flares occurred during the flights. Upper limits to the quiet time solar neutron fluxes at the 95% confidence level are ~~2.8, 4.6, 9.7~~ [.00028, .00046, .00096] and ~~9.0×10^{-4}~~ [.00090] neutrons/cm^2-sec in the energy intervals of 10-30, 30-50, 50-100 and 10-100 MeV, respectively.

(9) Technical rept.

*Present address, Department of Space Research, University of Birmingham, England.

A- DN 406495

(1) Upper Limits to the Quiet-Time Solar Neutron Flux from 10 to 100 MeV.

(10) Shin/Moon, George M./Simnett[redacted] R. Stephen/White

Department of Physics and Institute of Geophysics and Planetary Physics

University of California
Riverside, California

(11) 23 June[redacted]75

(12) 31 p.

(14) IGPP-UCP-75-15

(15) N00014-69-A-0200-5004[redacted], NGR-05-008-022

The UCR large area solid-angle double scatter neutron telescope was flown to search for solar neutrons on 3 balloon flights on September 26, 1971, May 14, 1972 and September 19, 1972. The first two flights were launched from Palestine, Texas and the third from Cape Girardeau, Missouri. The float altitude on each flight was at about 5 g/cm^2 residual atmosphere. Neutrons from 10 to 100 MeV were measured. No solar flares occurred during the flights. Upper limits to the quiet time solar neutron fluxes at the 95% confidence level are ~~2.8, 4.6,~~ .00028, .00046, ~~9.6~~ .00096 and ~~9.0 x 10^{-4}~~ .00090 neutrons/cm^2-sec in the energy intervals of 10-30, 30-50, 50-100 and 10-100 MeV, respectively.

(9) Technical rept.,

*Present address, Department of Space Research, University of Birmingham, England.

A-

DN 406495

I. INTRODUCTION

The measurement of neutrons from the sun during solar flares and quiet times will give important information about acceleration mechanisms on the sun. Following the early works of Giovanelli (1947) and Dungey (1958), the importance of magnetic field merging as a basic particle acceleration mechanism on the sun has been widely accepted (Sweet, 1958; Parker, 1963; Petschek, 1964; Syrovatskii, 1966a, 1966b; Sturrock, 1966, 1968). There is general agreement that solar flares derive their energy from sunspots and that this energy flows upward through the photosphere and chromosphere to the corona and is stored in magnetic fields or in particles trapped in magnetic fields. At the time of a flare, a fast transfer of energy is initiated that accelerates particles and produces electromagnetic radiation.

Magnetic field energy is transferred to charged particles by the merging of magnetic field lines at a line of magnetic neutral points (Giovanelli, 1947, 1948; Dungey, 1958; Sweet, 1958; Parker, 1963; Petschek, 1964). An electric field is set up along the neutral line that accelerates particles to high energies (Syrovatskii, 1966a, 1966b, 1969). Severny (1964) has suggested that a hot dense plasma at a temperature of [illegible] $\times 10^7$ °K and density of 10^{14} atoms/cm^3 is formed behind a shock front and that neutrons can be produced by thermonuclear reactions. Another possible flare mechanism that predicts large neutron fluxes is discussed by Elliot (1964, 1969, 1973) where trapped high energy protons are dumped rapidly into the sun's atmosphere.

Charged particles have not been useful for obtaining the initial times and energies of flares or accelerations to test these theories except at high latitudes because the charged particles do not penetrate the earth's magnetic field. Even with probes in interplanetary space or balloons at high geomagnetic latitudes the initial times and angles are lost and energies are distorted because of the interplanetary magnetic fields and magnetic irregularities. Neutrons, on the other hand, move unaffected by the interplanetary magnetic fields.

Solar electrons seldom reach energies above a few MeV because of large energy losses by bremsstrahlung and synchrotron radiation in the sun's atmosphere and magnetic field. Therefore, interplanetary electrons are not good indicators of the fundamental acceleration in solar flares. X-rays produced primarily by the bremsstrahlung of the electrons in the sun's atmosphere have the same limitations. Protons and heavier particles, however, lose energy only by ionization and collision losses. They attain much higher energies and transfer the initial fundamental information to the neutrons through nuclear collisions.

The solar neutrons produced by collisions of protons with He and other constituents of the sun's atmosphere can give important information about the time, energy and angular distributions of the accelerated protons. From the neutron measurements the potential that accelerates the protons and the time dependence of the acceleration may be deduced. Information about the electric field and its extent in the solar flare could thus be obtained. Direct information can be gained about the rate of the magnetic field merging and the dumping of protons trapped in the sun's magnetic field.

A number of authors have considered the secondary radiations that could be produced by the interactions of accelerated flare particles with the solar atmosphere. (Lingenfelter et al., 1965a,b; Dolan and Fazio, 1965; Lingenfelter and Ramaty, 1967; Lingenfelter, 1969; Chupp, 1971; Reppin et al., 1973a; Ramaty et al. 1975). The theoretical predictions of the solar neutron fluxes depend on the choice [illegible] the flare model for both the acceleration and slowing down of the char[illegible] particles. The numbers of high energy neutrons produced and their energy distributions are quite sensitive to the total number of accelerated protons and their rigidity spectra.

Lingenfelter et al. (1965b) have calculated the flux of neutrons expected near the earth. They include the loss from neutrons that decay in flight. For different values of the steepness of the proton rigidity spectra at the sun, the neutron distributions at the earth peak between 20 and 60 MeV. If the neutrons are released in a time short compared to the transit time to the earth, the sun-earth distance can act like a time-of-flight spectrometer with the highest energy neutrons arriving first.

The estimates by Lingenfelter and Ramaty (1967) of the neutron flux at 1 A.U. for the large flare of November 12, 1960 is 5-30 neutrons/cm^2-sec. Similarly, for the November 2, 1966 event, 0.1-0.4 neutrons/cm^2-sec were expected. If the optical emission from solar flares is provided by ionization losses of the accelerated particles in the flare, neutron fluxes of 8 neutrons/cm^2-sec arrive at the earth from the largest flares (3+) (Lingenfelter, 1969).

To date no neutrons have been seen from solar flares or from the quiet sun. However, the intensities and time histories of the 2.2 MeV gamma-rays observed during the August 4 and 7, 1972 flares by Chupp et al. (1973a,b) lead to estimates of fluxes at the earth of 20 neutrons/cm^2 and 30-50 neutrons/cm^2, respectively, in 3000 sec (Reppin et al., 1973a). A peak flux of 3 x 10^{-3} neutrons/cm^2-sec from 10-100 MeV is estimated for the

August 4 event, a flux that could easily have been measured with the University of California, Riverside (UCR) telescope. Preliminary upper limits to the quiet time neutron fluxes for September 26 and 27, 1971 have previously been reported. (White et al. 1973).

II. METHOD

The method of neutron detection has been described in detail by Grannan et al. (1972). The neutron's energy, scattering angle and flux are measured by two neutron scatters as shown in Figure 1. The incident neutron, n, with energy, E_n, scatters elastically from a proton in the liquid scintillator, S1. The recoil neutron, n_1, continues on and scatters from a proton or a carbon nucleus in the liquid scintillator, S2. The recoil proton energy, E_{p1}, in S1 is determined by pulse height analysis (PHA) of the light output. The recoil neutron energy, E_{n1}, is calculated from the measured time-of-flight (TOF) and the distance between the cells where the scatters occur.

From conservation of energy in neutron-proton scattering, E_n is given by

$$E_n = E_{p1} + E_{n1} \tag{1}$$

The scattering angle, α, is obtained from

$$\tan \alpha = \left(\frac{E_{p1}}{E_{n1}} \right)^{\frac{1}{2}} \tag{2}$$

Since the recoil proton direction is not measured, the incident neutron direction is determined to a cone of opening angle α.

A schematic cross-section of the neutron detector is shown in Figure

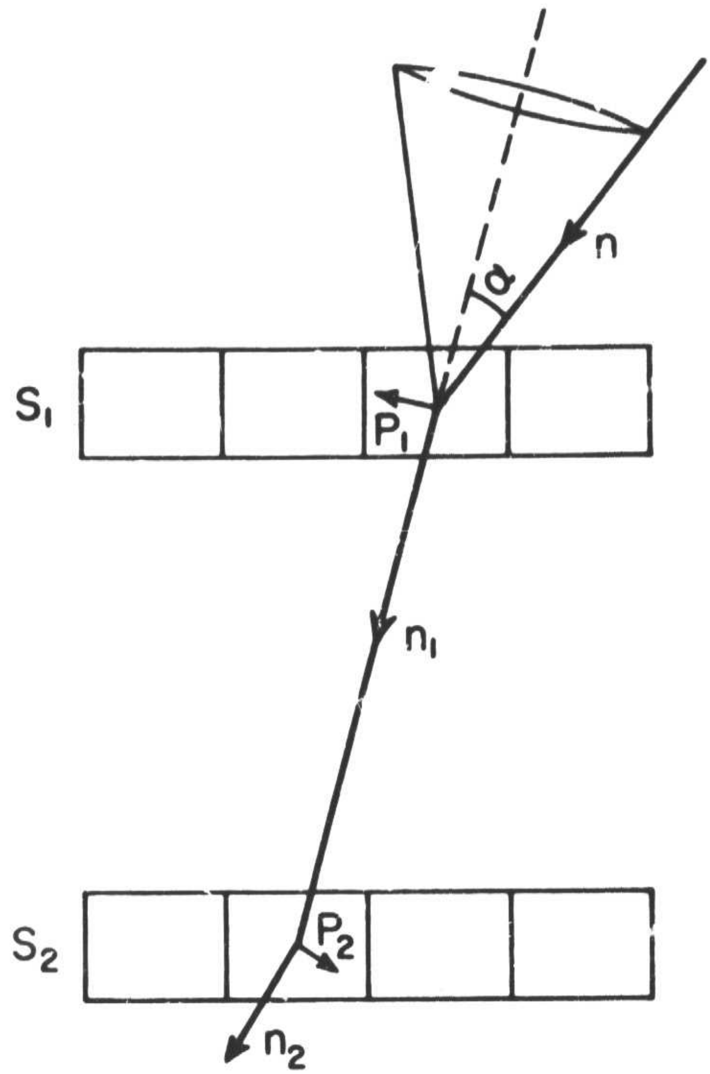

Figure 1.

2. The liquid scintillator is contained in the aluminum tanks, S1 and S2, 100 cm x 50 cm x 15 cm, 1 meter apart from center to center. They are equally divided into eight cells. Each tank is completely surrounded by a plastic scintillator (Pilot F). Each liquid scintillator cell is viewed by a 5 inch Amperex XP 1040 photomultiplier tube. The A_{11} and A_{21} plastic sheets are viewed by 5 inch Amperex XP 1040 tubes. The A_{12}, A_{22} and all side plastic sheets are viewed by 2 inch RCA 8575 tubes. The two liquid scintillator tanks are supported by four 6mm thick chromium-molybdenum steel tubes with 6.3 cm^2 cross-sections. The entire detector is contained in an aluminum gondola. The gondola has cylindrical walls of 3.2 mm thickness and 1.6 mm spherical end caps. It is sealed with a large O-ring and surrounded by 15 cm thick polystyrene to maintain the atmospheric pressure and room temperature. The incident downward moving neutrons must penetrate 2 g/cm^2 of material to reach the top liquid scintillator tank. The orientation of the detector relative to the sun was measured with 32 photo diodes placed on the outside wall of the gondola insulation.

The measured energy resolution, half width at half maximum, HWHM, is 12% at 15 MeV and 20% at 40 MeV and the calculated resolution is 20% at 100 MeV. The measured angular resolution HWHM is 10°.

The telescope efficiency $\varepsilon(E_n,\theta)$ for a point source of neutrons with energy E_n and angle θ is defined as the ratio of the detector count rate to the incident neutron flux. The efficiency $\varepsilon_{ij}(E_n,\theta)$ for one pair of cells, i and j, is found from

$$\varepsilon_{ij}(En,\theta) = N_H \cdot \left[\frac{d\sigma(E_n,\theta)}{d\Omega} \right]_{n,p} .$$

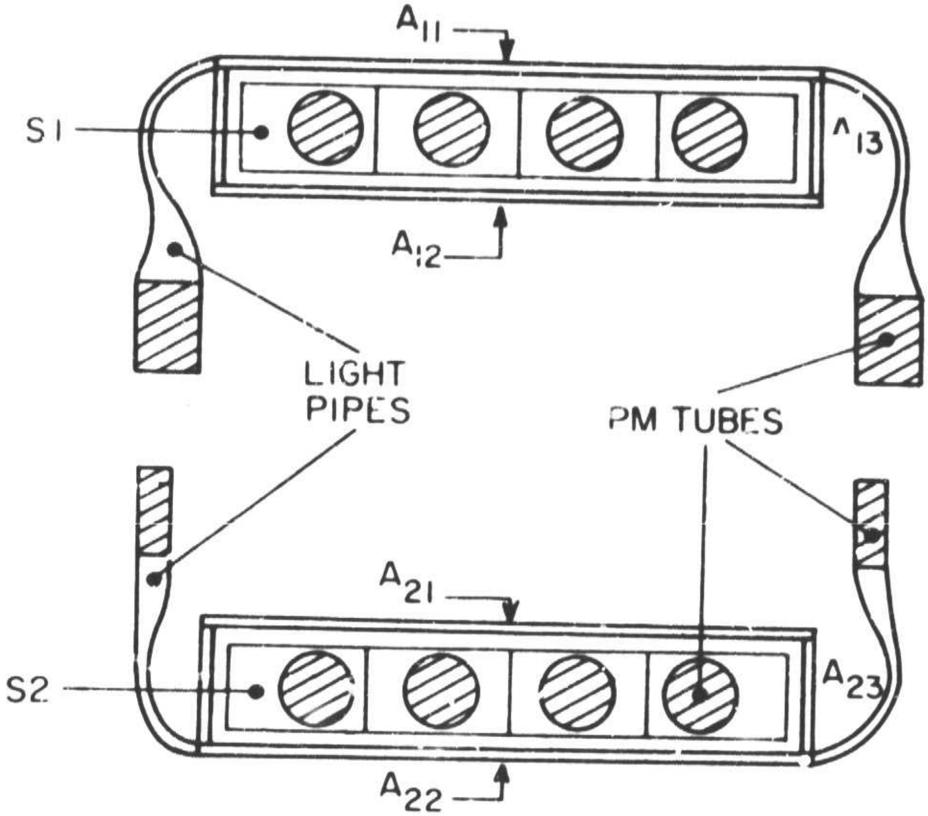

Figure 2.

$$\left[N_H\,\sigma_{np}(E_{n1})+N_C\,\sigma_{nc}(E_{n1})\right]\cdot f_o(E_n)\cdot f_1(E_{n1})\cdot\frac{V^2}{r^2} \qquad (3)$$

and the total detector sensitivity is the sum over all cells

$$\varepsilon(E_n,\theta) = \sum_{i,j=1}^{8} \varepsilon_{ij}(E_n,\theta) \qquad (4)$$

where i is a cell in S1 and j a cell in S2

E_n is the incident neutron kinetic energy.

θ is the incident zenith angle.

θ' is the scattering angle of the neutron-proton interaction in the S1 tank and depends on the azimuth angle of the incident neutron and the given pair of cells.

N_H is the number density of hydrogen atoms in the liquid scintillator, 7.04×10^{22} atoms/cm^3.

N_c is the number density of carbon atoms in the liquid scintillator, 4.19×10^{22} atoms/cm^3.

$f_o(E_n)$ is the fraction of incoming neutrons that survive after passing through the material from outside the gondola to the point of detection in S1.

$f_1(E_{n1})$ is the fraction of the neutrons scattered in S1 that survive to be detected in S2.

V is the volume of liquid scintillator in each cell.

r is the center to center distance between a pair of cells.

$\frac{d\sigma(E_n,\theta')}{d\Omega}{}_{n,p}$ is the differential scattering cross section for n-p scattering in S1 that gives a signal above threshold.

$\sigma_{np}(E_{n1})$ is the total cross section for n-p scattering in S2, evaluated at E_{n1}, that gives a signal above the threshold.

$\sigma_{nc}(E_{n1})$ is the inelastic cross section for neutron-carbon scattering in S2, evaluated at E_{n1}, that gives a signal above the threshold.

The penetration factors $f_o(E_n)$ and $f_1(E_{n1})$ are calculated from

$$f = e^{-N\sigma t} \tag{5}$$

where N is a number density of detector material, σ is the inelastic scattering cross section, and t is the thickness of the material.

The minimum detectable directional solar neutron flux F_{min} above background is determined by the efficiency ε, the minimum solid angle ΔΩ and observation time T. Let the background flux of downward moving atmospheric neutrons be B (n/cm^2-sec-sr), then the number of background counts in ΔΩ for T second is BεTΔΩ. A one standard deviation (σ) fluctuation in background counts is $(B\epsilon T\Delta\Omega)^{1/2}$. If we require the number of solar neutron counts to exceed the background fluctuation by a factor of 2, the minimum detectable solar neutron flux is

$$F_{min} = \frac{2}{f_s}\left(\frac{B\Delta\Omega}{\epsilon T}\right)^{1/2} \quad \text{neutron/cm}^2\text{-sec} \tag{6}$$

The f_s is the fraction of solar neutrons that can be identified within the resolution element ΔΩ. To estimate the minimum solar flux capability of the UCR neutron telescope, we use a B of 10^{-2} neutrons/cm^2-sec-sr in the neutron energy interval 10–100 MeV at 45° at an altitude of 4.9 gm/cm^2 and 40°N geomagnetic latitude (Preszler, 1973). A solid angle conical aperture gives $\Delta\Omega \approx 2.3$ ster and the corresponding correction factor f_s is 0.72. The detector sensitivity (area x efficiency) is about 24 cm^2 at 42 MeV. For an observation time of 10^4 sec this gives $F_{min} \approx 8.6 \times 10^{-4}$ n/cm^2-sec. More rigorous calculations, averaging over the backgrounds at all solid angles with efficiencies weighted by the expected solar neutron spectrum, give the values of Table 4.

III. DATA ANALYSIS

a) Balloon Flight Summary

The neutron detector was first launched on a 10.6 million cubic foot balloon from Palestine, Texas at 40°N geomagnetic latitude at 12:30 GMT on September 26, 1971. It reached the ceiling altitude of 5.0 gm/cm^2 in about two and a half hours. The detector remained at ceiling altitude from 14:50 GMT until 17:30 GMT the following day. The solar neutron data were accumulated during 5/8 of the time throughout the flight. A second balloon of 15 million cubic feet, was launched from Palestine, Texas at 12:48 GMT, the morning of May 14, 1972. The balloon floated at altitudes of 3.7 to 5.2 gm/cm^2 for 30 hours before termination. The third balloon, also 15 million cubic feet, was launched from Cape Girardeau, Missouri at 45°N geomagnetic latitude at 9:12 GMT on September 19, 1972. It remained at the ceiling altitude of 5 gm/cm^2 for about 24 hours.

No major solar flares or proton events occurred during the three balloon flights. Therefore we measured the quiet time solar neutron flux, only.

b) Identification of Solar Neutrons

The arrival direction of the incident neutrons are measured within a conical ring, which has a known projection in the celestial sphere. The cone for each event projects an event circle on the celestial sphere as shown in Figure 3. The recoil neutron path is determined by the cells in S1 and in S2 where the scatters occurred. The event cones are divided into two types, "vertical" and "cross", depending on the path. If the neutron scatters vertically downward from S1 to the corresponding cell in S2 the event is called a vertical event. The event circle produced by a vertical event has a fixed zenith angle that is identical to the neutron-proton scattering angle α in S1. Therefore, we can look for solar neutrons by comparing directly the zenith angles of the incident neutrons to the sun's zenith direction. We ask the question, "Do the zenith angles of the sun and of the incident neutron agree?"

If the recoil neutron direction is not vertically downward the event is called a cross event. The zenith angle of the event circle for a cross event depends on the scattering angle and the recoil neutron path. Since the incident direction is determined to a conical annulus, different directions along the cone have different zenith angles and thus the angle of scatter cannot be compared to the zenith angle of the sun as for the vertical events. For this case the minimum angle between a direction on the event cone and the sun's direction, δ, is useful, see Figure 3. It is necessary to define a source cone as the cone whose axis points toward the sun from the scatter point in S1. Its opening angle is adjusted as explained below. Any event cone with a minimum angle δ less than the half opening angle of

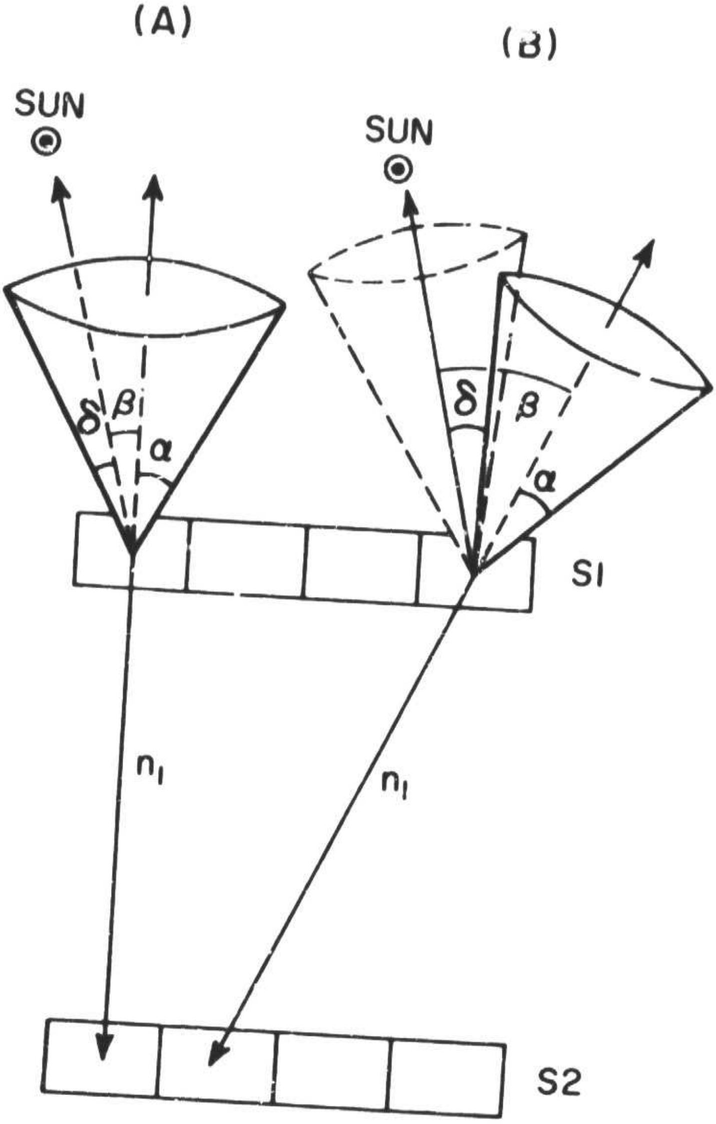

Figure 3.

the source cone intersects the source cone and is a candidate for a solar neutron event. The background of atmospheric neutrons whose event cones intersect the source cone is eliminated by subtracting the number of intersecting events when the sun is not in the field of view.

The opening angle of the source cone is adjusted to maximize the signal to noise ratio. The histogram of minimum δ's for 40 MeV neutrons (from the University of California, Davis cyclotron) incident on the detector at an angle of 45° is shown in Figure 4. From this curve it is found that 49%, 72% and 75% of the incident neutrons are included in half opening angles of 10° 15° and 20°, respectively. In the September 26, 1971 flight, the relative numbers of background atmospheric neutron event cones intersecting 10°, 15° and 20° source cones are 0.70, 1.00 and 1.27, respectively. The ratio of solar neutrons to the square root of the background neutrons normalized to the 15° cone for 10°, 15° and 20° source cones are 0.81, 1.00 and 0.92, respectively. Therefore, the source cone with half opening angle of 15° is the optimum cone.

In order to determine the minimum angle δ for each incident neutron, a coordinate system fixed on the detector is chosen so that the Z axis corresponds to the zenith of the celestial sphere as shown in Figure 5. The X-axis is the reference line from which the sun's azimuth is measured. The line element $\overline{OA}$ is the cone axis determined by the line that connects the first and second scattering points, assumed at the center of cells. θ_s is the zenith angle of the sun, θ_c the zenith angle of the cone axis, ϕ_s the azimuth angle of the sun and ϕ_c the azimuth of the cone axis. If we rotate the coordinate system about the Z-axis through an angle ϕ_c, then rotate the system about the new Y-axis through an angle θ_c, we arrive at Figure

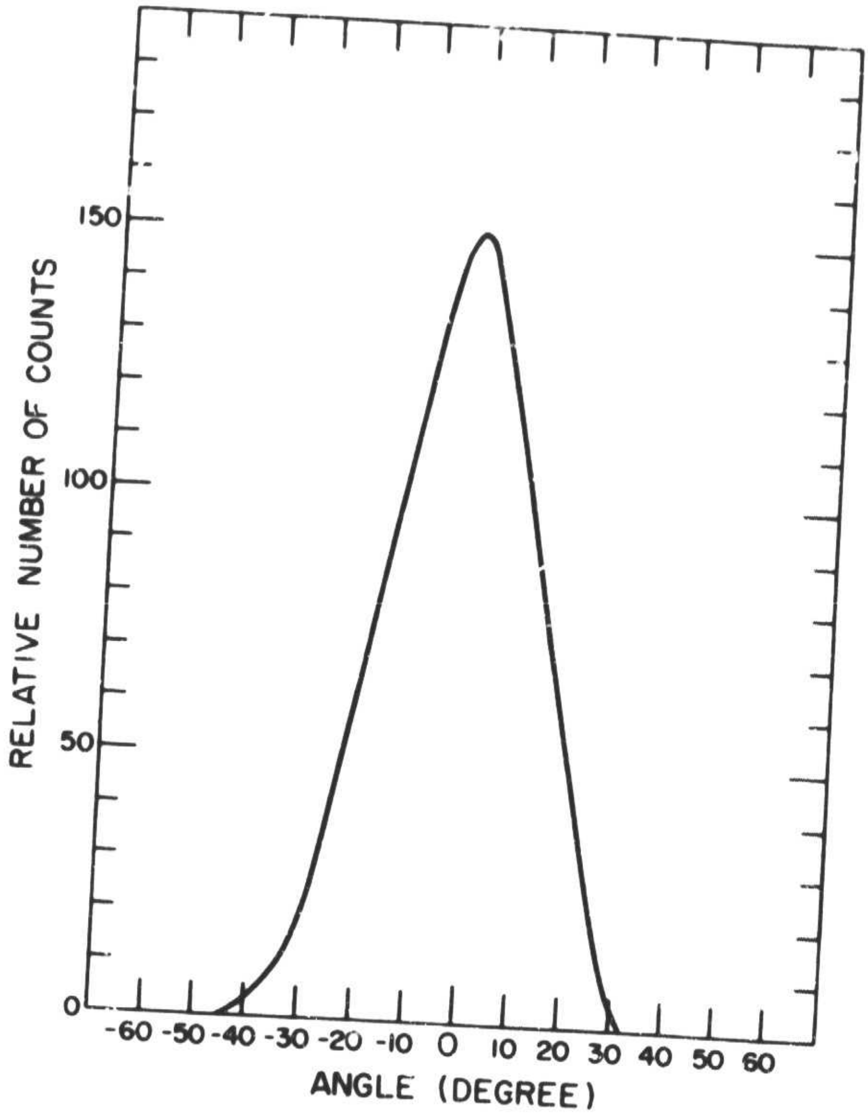
RELATIVE NUMBER OF COUNTS
150
100
50
0
-60 -50 -40 -30 -20 -10 0 10 20 30 40 50 60
ANGLE (DEGREE)

Figure 4.

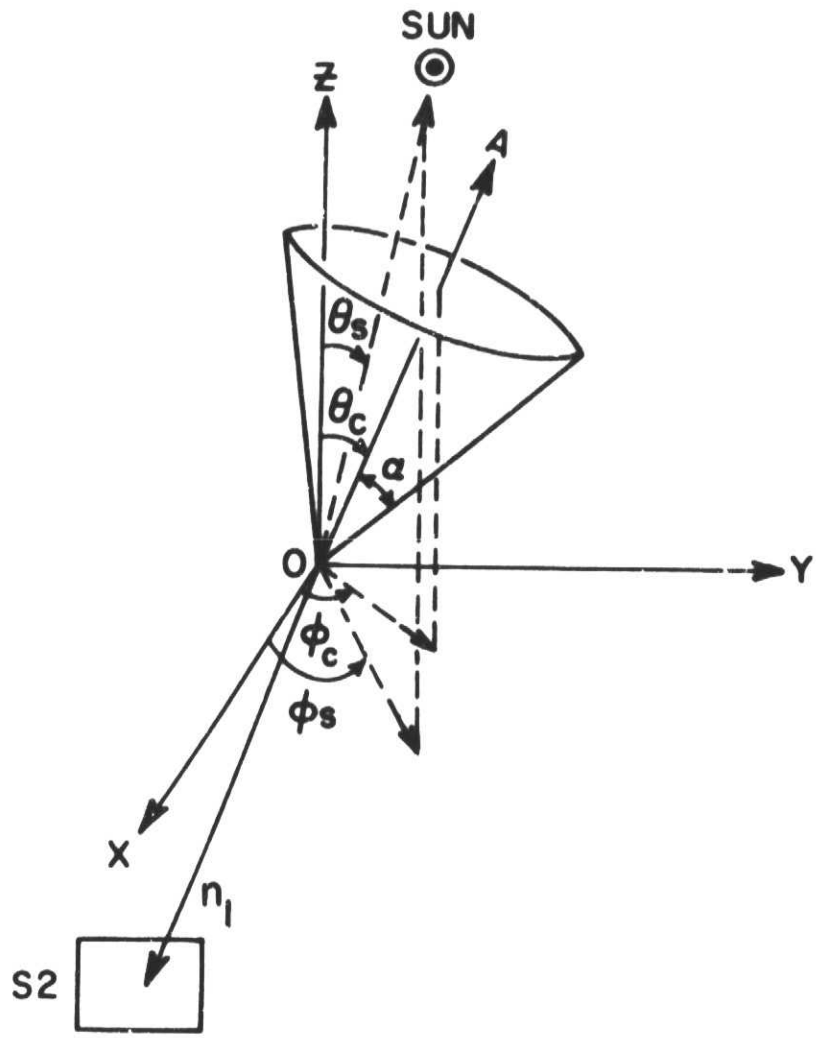

Figure 5.

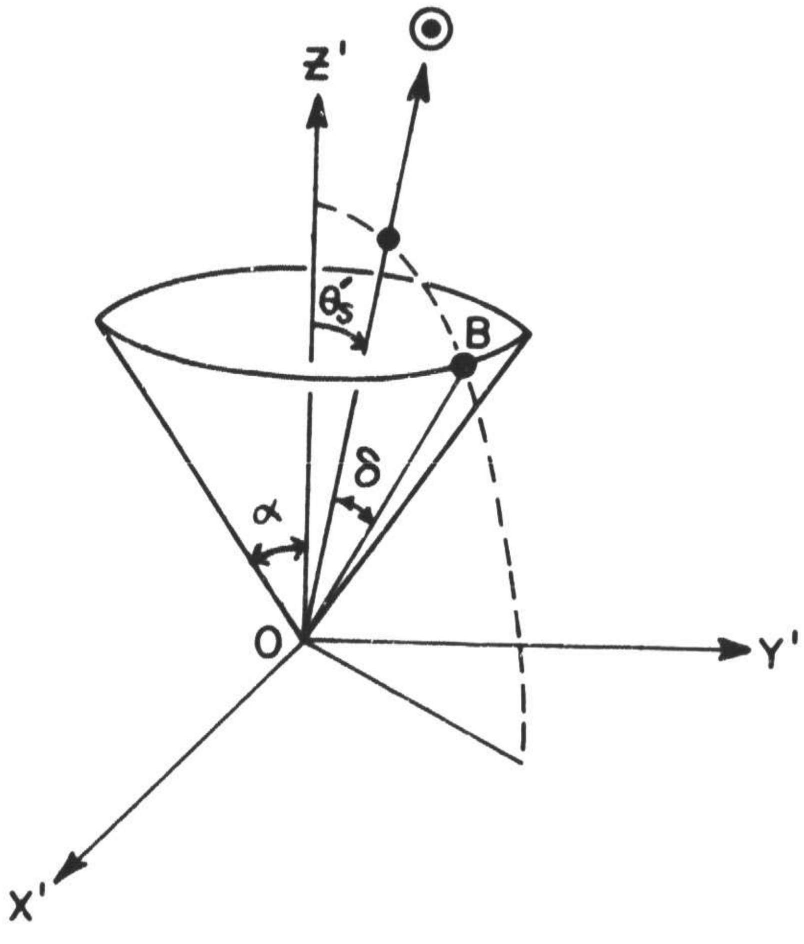

Figure 6.

6. In the new primed coordinate system, point B on the cone has the same azimuth angle as the sun. The minimum angle δ is the difference in zenith angle between the sun and the event cone in the new coordinate system.

Events with a start signal in S1, stop signal in S2 and a transit time greater than 7 ns are defined as solar mode neutron events. They consist of downward moving atmospheric neutrons and solar neutrons.

IV. RESULTS

The solar neutron fluxes, as calculated from the day-night differences of the vertical events, for the September 26, 1971 flight has been previously published (White et al. 1973). No statistically significant (above 2σ) solar fluxes were found. In that paper observations were presented for the sun at zenith angles from 31° to 50°. Since the vertical events were only 10% of the total events, the results for all data including both vertical and cross events are given here.

Data were analyzed event by event to find the minimum angle when the sun's zenith angle was 31°-50°. The observation time was 11,277 sec during the day and 17,527 sec during the night. At night the sun's position and the relative detector position are simulated under the assumption that the atmospheric background neutron flux is symmetric in azimuth. The counting rates for day and night are obtained by dividing the number of event cones intersecting the source cone of half opening angle 15° by the observation time. The count rates for vertical and cross events in four different

Table 1. Results of the September 26, 1971 flight from Palestine, Texas.

	Zenith Angle of the Sun	Neutron Energy (MeV)	'Day' Counting Rates s^{-1}	'Night' Counting Rates s^{-1}	(Day-Night)x10^{-3} s^{-1}
Vertical Events	31^o-50^o	20-30	0.0456 ± 0.0020	0.0409 ± 0.0015	4.7 ± 2.5
		30-50	0.0359 ± 0.0017	0.0341 ± 0.0014	1.7 ± 2.2
		50-100	0.0228 ± 0.0014	0.0230 ± 0.0011	-0.1 ± 1.8
		20-100	0.1044 ± 0.0030	0.0981 ± 0.0024	6.3 ± 15.1
Cross Events	31^o-50^o	10-30	0.2309 ± 0.0045	0.2388 ± 0.0036	-7.9 ± 5.8
		30-50	0.1372 ± 0.0077	0.1353 ± 0.0027	1.9 ± 8.1
		50-100	0.1338 ± 0.0034	0.1420 ± 0.0028	-8.2 ± 4.4
		10-100	0.5020 ± 0.0066	0.5162 ± 0.0054	-14.2 ± 8.6
Total	31^o-50^o	10-100	0.6733 ± 0.0077	0.6743 ± 0.0062	-1.0 ± 9.9

energy ranges are given in Table 1. The errors for day and night are statistical and obtained by dividing the square root of the counts in each energy interval by the measurement time. The day-night difference is obtained by subtracting the nighttime counting rate from the daytime counting rate. No statistically significant solar flux at a confidence level of 95% was observed.

On the May 14, 1972 flight the high voltage power supplies for the photomultiplier tubes viewing the anticoincidence system were partially disabled during the flight. Therefore, the counting rates are higher than the earlier flight launched at the same geomagnetic latitude. The charged particle leakage backgrounds are eliminated when the nighttime counting rate is subtracted from the daytime counting rate. In Table 2, the diurnal counting rate shows no statistically significant solar neutron flux at a confidence level of 95%.

The results from the September 19, 1972 flight are given in Table 3. No statistically significant solar neutron fluxes were observed at a confidence level of 95%.

Since no positive solar neutron fluxes from the quiet Sun were measured throughout the three separate experiments, the upper limits for the quiet time solar neutron fluxes are quoted at a 95% confidence level (2σ) from the following relation

$$F_s \leq \frac{2}{\epsilon . f_s} \left(\frac{N_d}{T_d^{\,2}} + \frac{N_n}{T_n^{\,2}} \right)^{\frac{1}{2}} \qquad (7)$$

Table 2. Results of the May 14, 1972 flight from Palestine, Texas.

	Zenith Angle of the Sun	Neutron Energy (MeV)	'Day' Counting Rates s^{-1}	'Night' Counting Rates s^{-1}	(Day-Night)x10^{-3} s^{-1}
Vertical Events	30^o-50^o	10-30	0.1056 ± 0.0043	0.1043 ± 0.0013	+1.3 ± 4.5
		30-50	0.0441 ± 0.0028	0.0485 ± 0.0031	-4.3 ± 4.3
		50-100	0.0329 ± 0.0024	0.0376 ± 0.0029	-4.7 ± 3.8
		10-100	0.1826 ± 0.0057	0.1904 ± 0.0065	-7.7 ± 8.7
Cross Events	30^o-50^o	10-30	0.3552 ± 0.0080	0.3642 ± 0.0089	-9.0 ± 12.0
		30-50	0.2057 ± 0.0061	0.2309 ± 0.0071	-25.1 ± 9.4
		50-100	0.1990 ± 0.0060	0.2047 ± 0.0067	-5.6 ± 9.0
		10-100	0.7600 ± 0.0117	0.7998 ± 0.0133	-39.8 ± 17.7
Total	30^o-50^o	10-100	0.9427 ± 0.0130	0.9903 ± 0.0148	-47.5 ± 19.8

Table 3. Results of the September 19, 1972 flight from Cape Giradeau, Missouri.

	Zenith Angle of the Sun	Neutron Energy (MeV)	'Day' Counting Rates s^{-1}	'Night' Counting Rates s^{-1}	(Day-Night)x10^{-3} s^{-1}
Vertical Events	30°-50°	20–30	0.1062 ± 0.0028	0.1031 ± 0.0028	3.0 ± 4.0
		30–50	0.1107 ± 0.0029	0.1097 ± 0.0029	1.0 ± 4.1
		50–100	0.1233 ± 0.0031	0.1286 ± 0.0031	-5.3 ± 4.4
		20–100	0.3403 ± 0.0051	0.3416 ± 0.0051	-1.2 ± 7.3
Cross Events	30°-50°	10–30	0.8560 ± 0.0080	0.8628 ± 0.0079	-6.7 ± 11.3
		10–50	0.4975 ± 0.0061	0.5069 ± 0.0061	-9.3 ± 8.6
		50–100	0.7283 ± 0.0073	0.7446 ± 0.0074	-16.2 ± 10.4
		10–100	2.0819 ± 0.0125	2.1143 ± 0.0125	-32.3 ± 17.6
Total	30°-50°	10–100	2.5779 ± 0.0139	2.6071 ± 0.0138	-29.1 ± 19.6

Table 4. Upper Limits to the Solar Neutron Flux from the Quiet Sun.

(neutrons/cm^2-sec)

Energy (MeV)	Sept. 26, 1971	May 14, 1972	Sept. 19, 1972	Total
10–30	3.5×10^{-4}	6.7×10^{-4}	6.4×10^{-4}	2.8×10^{-4}
30–50	5.7×10^{-4}	11.6×10^{-4}	10.6×10^{-4}	4.6×10^{-4}
50–100	11.5×10^{-4}	22.8×10^{-4}	26.0×10^{-4}	9.6×10^{-4}
10–100	1.12×10^{-3}	2.2×10^{-3}	2.0×10^{-3}	9.0×10^{-4}

where F_s is the solar neutron flux in units of neutrons/cm^2-sec

N_d is the number of daytime neutron counts.

N_n is the number of nighttime neutron counts.

T_d is the daytime observation time.

T_n is the nighttime observation time.

$S=\epsilon A$ is the efficiency of the detector in units of effective area.

f_s is the fraction of solar neutrons identified within minimum angles of $\pm 15^o$.

The upper limits (2σ) to the solar neutron flux for the three flights and overall combined results are shown in Table 4. The combined result of the three experiments is given in the last column. The upper limit to the solar neutron flux from the quiet Sun from the three balloon flights in the energy interval of 10 to 100 MeV is 1.0×10^{-5} neutrons/cm^2-sec-MeV.

A list of attempts since 1966 to measure solar neutron fluxes from solar flares or the quiet sun are given in Table 5. Although Daniel et al. (1967, 1971) reported measuring neutrons from a sub flare, in no case is there convincing evidence that solar neutrons have been seen. Calculations of Roelof (1966) and Holt (1967) set upper limits assuming that protons measured in interplanetary space all arise from neutron decays. While these calculations give low limits to the solar neutron fluxes they are dependent on particular models for proton diffusion in interplanetary space. Such models decrease the estimated upper limits for the neutron fluxes significantly over the fluxes for no diffusion. And they do not calculate neutron fluxes from protons arising from neutron decays on the East limb of the sun, e.g., as these protons often cannot reach the vicinity of the earth.

The measurements of the upper limits for solar neutrons from the quiet

Table 5. Previous Measurements of Neutrons from the Sun

Reference	Method	Platform	Neutron Inten. (n/cm^2-sec) Quiet Sun	Solar Flare	Energy Interval (MeV)
Hess & Keiffer (1967)	BF_3 Moderated	OSO I	$<2x10^{-3}$		Ther. [illegible]-10
Haymes (1964)	Phoswich pulse shape discriminator	balloon below $4g/cm^2$	<0.02		1-14
Bame & Asbridge (1966)	He^3 gas-polyethylene moderator	Vela 1,2,3.	<0.01	<1 3B flare	1-20
Apparao et al. (1966) Daniel, personal communication (1974)	Nuclear Emulsions	balloon below $10g/cm^2$	<0.0148		20-160
Roelof (1966)	Compare to protons at 1 A.U.		$<2x10^{-4}$		20-80
Daniel et al. (1967,1971)	Scintillator spark chamber	balloon below $10g/cm^2$		$2.5x10^{-3}$ sub flare	50-500
Webber & Ormes (1967)	Compare to protons	balloon below $10g/cm^2$	<0.0024		>100
Holt (1967)	Compare to protons at 1 A.U.			<0.03 most favorable $<3x10^{-4}$ more typical	>50
Zych & Frye (1969)	Spark Chamber	balloon below $7g/cm^2$		$<1.0x10^{-2}$ Imp 1 Flare $<1.7x10^{-4}$ Imp 1 Flare	12-100
Forrest & Chupp (1969)	Plastic Scintillator	balloon below $4g/cm^2$	$<2x10^{-2}$	$<4x10^{-2}$ 1B flare	15-120
Daniel et al. (1969)	Plastic Scintillator	balloon below $25g/cm^2$		$<1.2x10^{-2}$ 2B flare	15-150
Heidbreder et al. (1970)	Double scattering from hydrogen in a spark chamber	balloon below $7g/cm^2$	$<1.25x10^{-3}$		100-400
Cortellessa et al. (1971)	Proton recoil-plastic scintillator	balloon below $4.5g/cm^2$	$<5.5x10^{-3}$		10-200
Kim (1970)	Proton recoil-nuclear emulsions	balloon below $6.6g/cm^2$	<2.5x10-2		20-160
Ryles et al. (1972)	Proton recoil-scintillator	balloon below $3g/cm^2$	$<5x10^{-3}$		50-350
Kirsch (1973)	Sea level neutron monitors			0.01	>50
Lockwood et al. (1973)	Moderated He^3 detector	OGO-6	$<1.8x10^{-3}$		1-20
White et al. (1973)			$<1.0x10^{-3}$		20-60
This Paper (1975)	Double scattering using pulse height and time of flight	balloon below $4.6g/cm^2$	$<2.8x10^{-4}$ $<4.6x10^{-4}$ $<9.6x10^{-4}$ $<9.0x10^{-4}$		10-30 30-60 50-100 10-100

sun are given in Figure 7. In the energy region of 20 to 60 MeV, where the greatest number of neutrons are expected from the sun, our upper limits are a factor of 10 lower than previous values. Further measurements with longer observation times on balloons or satellites will permit the detection and measurement of the properties of neutrons from solar flares. These longer observation times will also make possible the detection of neutrons from the quiet sun or decrease the upper limits significantly.

V. ACKNOWLEDGMENTS

We wish to thank Office of Naval Research Contract N00014-69-A-0200-5004 and NASA Grant NGR-05-008-022 for support of this work. We are also grateful to Dr. Allen Zych and Dr. Alan Preszler for many helpful conversations.

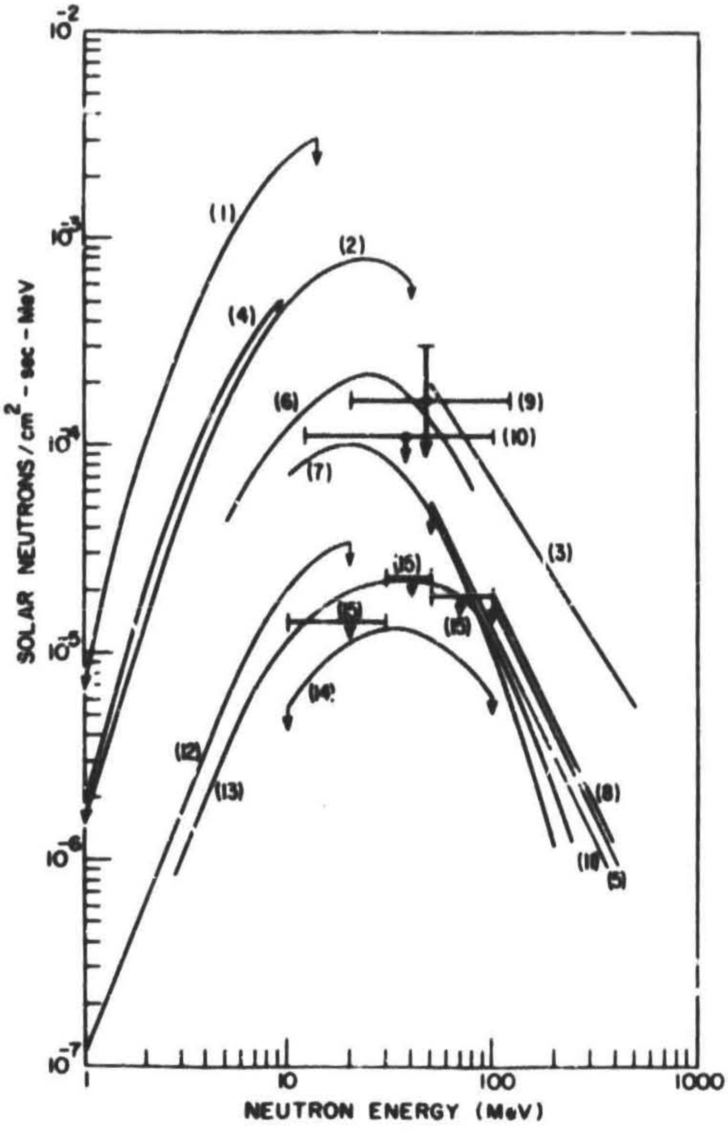

SOLAR NEUTRONS / cm² - sec - MeV
NEUTRON ENERGY (MeV)
(1)
(2)
(3)
(4)
(5)
(6)
(7)
(8)
(9)
(10)
(12)
(13)
(14)
(15)
(16)

Figure 7.

REFERENCES

Apparao, M. V. K., Daniel, R. R. and Vijayalaskahmi, B. 1966, J. Geophys Res., 71, 1781.

Bame, S. J., and Asbridge, J. R. 1966, J. Geophys. Res., 71, 4605.

Chupp, E. L. 1971, Space Sci. Rev., 12, 486.

Chupp, E. L., Forrest, D. J., Higbie, P. R., Suri, A. N., Tsai, C. and Dunphy, P. P. 1973a, Nature, 241, 333.

Chupp, E. L., Forrest, D. J., Suri, A. N. and Reppin, C., 1973b, 13th Intl. Cosmic Ray Conf., Denver, 1595.

Cortellessa, P., Di Benedetto, P. and Paizis, C. 1970, Solar Phys. 14, 427.

Daniel, R. R., Joseph, G., Lavakare, P. J. and Sunderrajan, R. 1967, Nature, 213, 21.

Daniel, R. R., Gokhali, S., Joseph, G., Lavakare, P. J. and Sekhon, B. S. 1969. Solar Phys., 10, 465.

Daniel, R. R., Gokhali, G. S., Joseph, G. and Lavakare, P. J 1971, J. Geophys. Res., 76, 3152.

Dolan, J. F. and Fazio, G. G. 1965, Rev. Geophys., 3, 319.

Dungey, J. 1958, Proc. IAU Symp. of Electromagnetic Phenomena in Cosmical Physics, Cambridge Univ. Press, 139.

Elliot, H. 1964, Planet. Space Sci., 12, 657.

Elliot, H. 1969, Solar Flares and Space Research, 356.

Elliot, H. 1973, Goddard Symposium Proceedings, 1972, Ed. Ramaty and Stone, NASA SP-342.

Eyles, C. J. Linney, A. D. and Rochester, G. K. 1972, Solar Phys. 24, 483.

Forrest, D. J. and Chupp, E. L. 1969, Solar Phys. 6, 339.

Grannan, R. T., Koga, R., Millard, W. A., Preszler, A. M., Simnett, G. M. and White, R. S. 1972, Nuclear Instruments and Methods 103, 99.

Giovanelli, R. G. 1947, Monthly Not. Roy. Astron. Soc., 107, 338.

Haymes, R. C. 1964, J. Geophys. Res., 69, 853.

Heidbreder, E., Pinkau, K., Reppin, C. and Schönfelder, V. 1970, J. Geophys. Res., 75, 6347.

Hess, W. N. and Kaifer, R. C. 1967, Solar Phys., 2, 202.

Holt, S. S. 1967, J. Geophys. Res., 72, 3507.

Kim, C. Y. 1970, Canadian J. Phys., 48, 2155.

Kirsch, E. 1973, Solar Phys., 28, 233.

Lingenfelter, R. E. and Flamm, E. J. 1964, Sci., 144, 292.

Lingenfelter, R. E., Flamm, E. J., Canfield, E. H. and Kellman, S. 1965a, J. Geophys. Res., 70, 4077.

Lingenfelter, R. E., Flamm, E. J., Canfield, E. H. and Kellman, S. 1965b, J. Geophys. Res., 70, 4087.

Lingenfelter, R. E. and Ramaty, R. 1967, High Energy Reactions in Astrophysics, Ed. B. S. P. Shen, W. A. Benjamin, Inc., N.Y., p. 99.

Lingenfelter, R. E. 1969, Solar Phys., 8, 341.

Lockwood, J. A., Ifedeli, S. O. and Jenkins, R. W. 1973, Solar Phys., 30, 183.

Parker, E. N. 1963, Astrophys. J. Suppl., 8, 177.

Petschek, H. E. 1964, AAS-NASA Symp. on the Physics of Solar Flares, NASA-SP-50, 425.

Preszler, A. M. 1973, Thesis, University of California, Riverside, California, "Earth Albedo Neutrons from 10 to 100 MeV."

Ramaty, R., Kozlovsky, B. and Lingenfelter, R. E., to be published in Space Science Reviews, 25, 461 (1975).

Reppin, C., Chupp, E. L., Forrest, D. J. and Suri, A. N. 1973a, 13th Intl. Cosmic Ray Conf., Denver, 1577.

Roelof, E. C. 1966, J. Geophys. Res. 71, 1305.

Sturrock, P. A. 1966, Nature, 211, 695.

Sturrock, P. A., 1968, Proc. IAU Symp., Reidel, Dordrecht, Holland, 35, 465.

Sweet, P. A. 1958, Nuovo Cimento, Suppl. 8, 2, 188.

Syrovatskii, S. I. 1966a, Astron. Z. USSR, 43, 340.

Syrovatskii, S. I. 1966b, J. Exp. Theor. Phys., 50, 1133.

Syrovatskii, S. I. 1969, Solar Flares and Space Res., North-Holland, Amsterdam, 346.

Webber, W. R. and Ormes, J. F. 1967, J. Geophys. Res., 72, 3387.

White, R. S., Moon, S., Preszler, A. M. and Simnett, G. M. 1973, Space Research XIII, Ed. M. J. Rycroft and S. K. Runcorn, Akademie-Verlag, Berlin, 2, 683.

Zych, A. D. and Frye, G. M. 1969, J. Geophys. Res., 74, 3726.

FIGURE CAPTIONS

Figure 1. Schematic view of a double scattering neutron event. The incident neutron direction is determined to a cone of half opening angle α.

Figure 2. A schematic section through the detector system. The two liquid scintillator tanks S1 and S2, the plastic anti-scintillators A11, A13, A12, A21, A23 and A22, the photo-multipliers and the light pipes are shown.

Figure 3. Examples of event cones and a source cone. The source cone is shown with dotted lines. The vertical and the cross events are determined by the direction of the recoil neutron n_1. β is the angle between the Sun's direction and the source cone axis. α is the half opening angle between a direction on the event cone and the sun's direction. δ is the minimum angle between a direction on the event cone and the sun's direction.

Figure 4. A curve of the distribution of minimum angles δ for 40 MeV neutrons. $\delta = \alpha - \beta$ where α is a half opening angle of an event cone and β is the angle between the event cone axis and the source direction. (See Figure 3.)

Figure 5. A coordinate system fixed on the detector. The center of the cell in S1 where the first scattering takes place is the origin O of the coordinate system.

Figure 6. The minimum angle $\delta = \theta_s' - \alpha$ is shown in the rotated coordinate system in which the cone axis corresponds to the Z axis.

Figure 7. Upper Limits to quiet time solar neutron fluxes. The curves are identified by (1) Haymes, 1964, (2) Bame and Asbridge, 1966, (3) Daniel et al., 1967, 1971, (4) Hess and Kaifer, 1967, (5) Webber and Ormes, 1967, (6) Forrest and Chupp, 1969, (7) Cortellessa et al., 1971, (8) Heidbreder et al., 1970, (9) Kim, 1970, (10) Zych and Frye, 1968, (11) Eyles et al., 1967-69, (12) Lockwood et al., 1969, (13) Lingenfelter and Flamm, 1964, (14) Present Work (10-100 MeV), and (15) Present Work (10-30, 30-50, 50-100 MeV).